Electronic Supplementary Material (ESI) for Journal of Materials Chemistry C.

Electronic Supporting Information

Insight into the Aggregation Prospective of Schiff Base AIEgens Enabling Efficient Hydrazine Sensor in their Aggregated State

Senjuti Halder,[a] Biswajit Nayak, [a] Basu Bhattacharjee,[b] Aiyagari Ramesh*[b] and Gopal Das *[a]

[a.] Department of Chemistry, Indian Institute of Technology Guwahati, Guwahati 781039, Assam, India. E-mail: gdas@iitg.ac.in

[b] Department of Biosciences and Bioengineering, Indian Institute of Technology Guwahati, Guwahati 781039, Assam, India. E-mail: aramesh@iitg.ac.in

Materials and Experimental Methods: All the materials for synthesis and experiments were purchased from commercial suppliers and used without further purification.

Stock solutions of **1** and **2** (5×10^{-3} mol L^{-1}) was prepared in DMSO and then diluted to 10×10^{-6} mol L^{-1} for various spectral studies for aggregation behavior and sensing phenomenon in Millipore water and acetonitrile. The absorption measurements were recorded on a PerkinElmer Lamda-25 UV−Vis spectrophotometer using 10 mm path-length quartz cuvettes in the wavelength range of 300−700 nm while the fluorescence spectra were recorded on a Horiba Fluoromax-4 Spectrofluorometer using 10 mm path length quartz cuvettes with a slit width of 3 nm at 298 K. Mass spectrum of **1** and **2** were obtained using Waters Q-ToF Premier mass spectrometer. Nuclear magnetic resonance (NMR) spectra were recorded on a Bruker Advance 600 MHz instrument. The chemical shifts were recorded in parts per million (ppm) on the scale. The following abbreviations are used to describe spin multiplicities in ^{1}H NMR spectra: s = singlet; d = doublet; t = triplet; q= quartet, m = multiplet. The particle sizes were measured by dynamic light scattering (DLS) experiments on Malvern Zetasizer Nano ZS instrument equipped with a 4.0 mW He–Ne laser operating at a wavelength of 633 nm. The samples and the background were measured at room temperature (25 °C). The solution was equilibrated for 60 minutes before taking the measurements. To investigate the interaction with hydrazine on aggregation behavior of **1** and **2** individually, the concentration of the respective compound was maintained at 10 μM and hydrazine and other amine based compounds at 100 μM in final solutions for all spectral studies.

Detection Limit: The detection limit was calculated on the basis of the fluorescence titration. The fluorescence emission spectrum of **1** and **2** was measured 10 times, and the standard deviation of blank measurement was estimated. To measure the slope, the fluorescence emission at respective wavelength was plotted as a function of the concentration of hydrazine from the titration experiment. The detection limit was then calculated using the following equation:

$$\text{Detection limit} = 3\sigma/k \ldots (1)$$

Where σ is the standard deviation of blank measurement, and k is the slope between the fluorescence emission intensity versus $[N_2H_4]$.

Crystallography: The intensity data were collected using a Bruker SMART APEXII CCD diffractometer, equipped with a fine focus 1.75 kW sealed tube Mo-Kα radiation (λ= 0.71073Å)

at 298(2) K, with increasing ω (width of 0.3° per frame) at a scan speed of 3s per frame. The SMART software was used for data acquisition. Data integration and reduction were performed with SAINT and XPREP [1] software. Multi-scan empirical absorption corrections were applied to the data using the program SADABS [2]. Structures were solved by direct methods using SHELXL-2016/6 and were refined by full-matrix least squares on F_2 using SHELXL-2016/6 program package [3,4]. In the crystal structure, non-hydrogen atoms were refined aniso-tropically. Structural illustrations have been generated using MERCURY 2.3 for Windows [5]. CCDC no: 2062591, Empirical formula: C_{27} H_{24} N_2 O, Mw: 392.48, T= 298(2) K, Triclinic, space group: P -1, a= 8.3383(4) Å, b= 15.9039(8) Å, c= 16.4937(9) Å, α= 102.590(4), β= 104.008(4), γ= 92.454(4), V= 2060.60(19)Å^3, Z= 4, Dx(g/cm^3)= 1.265, F(000)= 832, Reflections collected/unique= 9344/ 5811, R_1= 0.0700, wR_2= 0.203 [I>2sigma(I)], R_1= 0.1104, wR_2= 0.2520 (all data), GOF(F2)= 0.841.

Fluorescence Microscopy: The samples **1** and **2** (1 mM) on increasing water in water-acetonitrile medium were prepared freshly by casting all preparation drops(5 μl) on a glass slide and were dried completely at room temperature followed by image acquisition using a fluorescence microscope (Eclipse Ti-U, Nikon, USA). Plant imaging were also conducted using the same instrument.

Field Emission Scanning Electron Microscopy: The morphology of the aggregated species and hydrazine interaction were investigated by using FESEM imaging studies by drop (1 mM/ 2 μl) cast method on glass plates covered with Al-foil using Gemini 300 FESEM (Carl Zeiss).

Atomic Force Microscopy: Transformations of aggregates due to hydrazine interaction were observed from a drop-cast solution of **1** and **2** (10 μM) in a 1:1 acetonitrile–water medium using Asylum Research Cypher (Oxford Instruments).

Density Functional Theory (DFT) Study: DFT optimizations of **1** and **2** were carried out with the RB3LYP/ 6-31G method basis set using the Gaussian 09 program where calculated total energy is -1228.03257060 a.u. and -1151.54328176 a.u respectively.

Cytotoxicity Assay for AIEgen 1 and 2: The cytotoxic effect of **1** and **2** on cultured HeLa cells was ascertained by a standard MTT assay. MTT (3-(4,5-Dimethylthiazol-2-yl)-2,5-Diphenyltetrazolium Bromide) solution was procured from Sigma-Aldrich, USA. HeLa cells were

initially propagated in 25 cm^2 tissue culture flask in Dulbecco's modified Eagle medium (DMEM) supplemented with 10% (v/v) fetal bovine serum (FBS), penicillin (100 μg/mL) and streptomycin (100 μg/mL) at 37 ^{0}C in a CO_2 incubator. Prior to MTT assay, cells were seeded onto 96-well tissue culture plates (approximately 10^4 cells per well) and incubated in separate sets with various concentrations of **1** and **2** (2.5 μM, 5.0 μM, 10 μM and 20 μM) made in DMEM for a period of 24 h at 37 ^{0}C in a CO_2 incubator. The control sample consisting of untreated HeLa cells was also incubated in parallel under the same conditions. Following 24 h incubation, the media was aspirated and fresh DMEM containing MTT solution was added to the cells and incubated for 4 h at 37 ^{0}C in a CO_2 incubator. Following incubation, the MTT solution was removed and the insoluble and colored formazan product was solubilized in DMSO. The absorbance of the solution was then measured in a microtiter plate reader (Infinite M200, TECAN, Switzerland) at 570 nm against a reference of 640 nm. MTT assay for every sample was performed in six sets. The absorbance obtained for the untreated control samples represented 100% cell viability. The absorbance obtained for **1**- or **2**-treated cells was compared to the control to ascertain the % cell viability.

Cell Imaging Studies: HeLa cells were initially propagated in 25 cm^2 tissue culture flask in Dulbecco's modified Eagle medium (DMEM) supplemented with 10% (v/v) fetal bovine serum (FBS), penicillin (100 μg/mL) and streptomycin (100 μg/mL) at 37 ^{0}C in a CO_2 incubator. Prior to cell imaging studies, HeLa cells were seeded into confocal dish (20 mm diameter) and grown in DMEM medium at 37 ^{0}C in a CO_2 incubator to achieve nearly 75% confluency. Subsequently the cells were incubated in separate sets with 10 equiv. hydrazine in DMEM at 37 ^{0}C for 10 min in a CO_2 incubator. DMEM medium was then aspirated and the cells were gently washed with sterile PBS in order to remove excess hydrazine and to each set, the AIEgens **1** and **2** (2.5 μM each) were added separately in DMEM and the cells were further incubated at 37 ^{0}C for 10 min in a CO_2 incubator. The cells were washed again with sterile PBS to remove excess ligand and their images were captured using a confocal microscope (Zeiss LSM 880, Germany). The excitation wavelength used for the lasers encompassed 488 nm for green emission, 405 nm for blue emission and 561 nm for red emission. Images for HeLa cells incubated with either **1** or **2** alone was also captured.

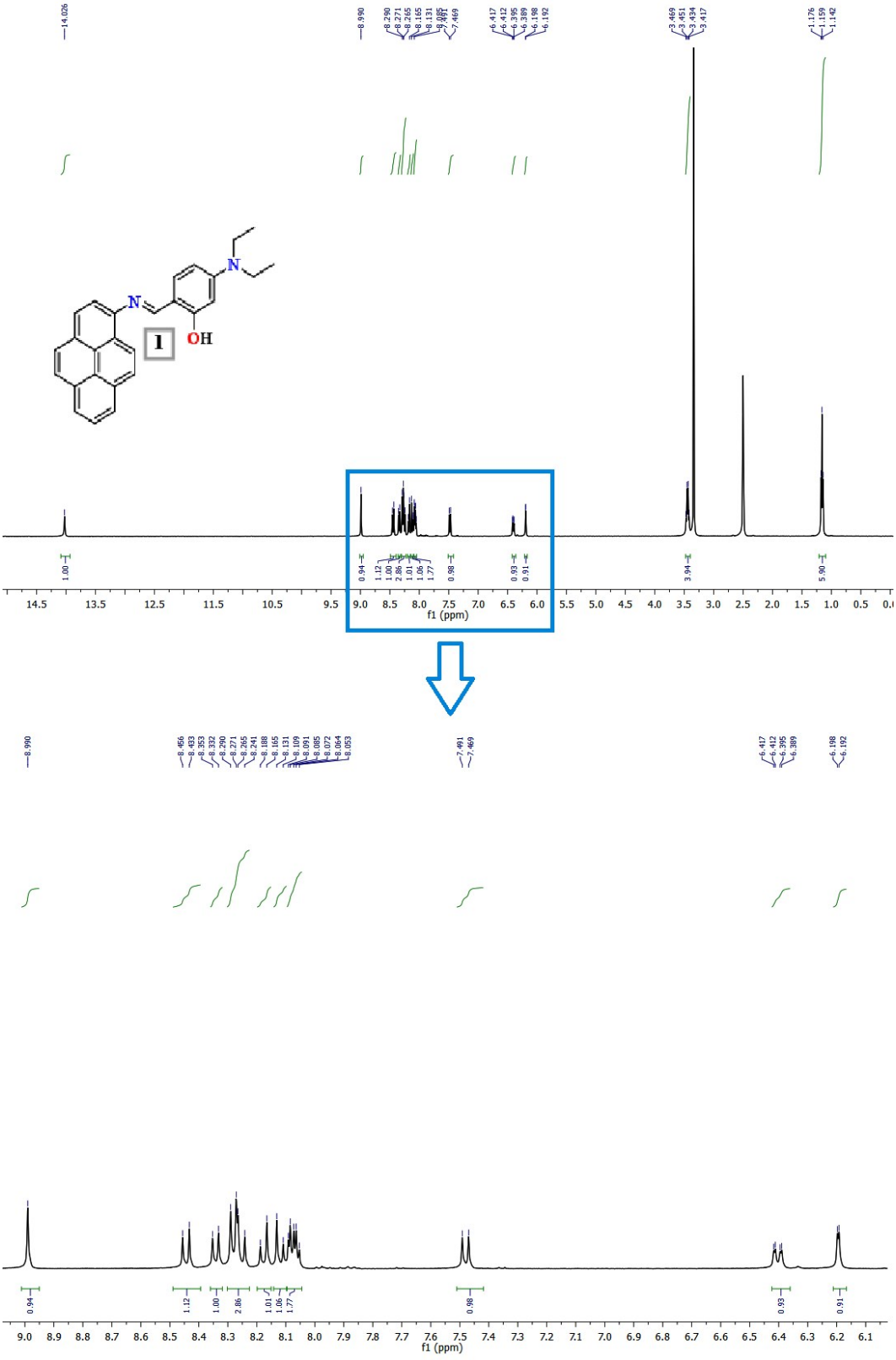

Figure S1: ^{1}H-NMR spectra of **1** in DMSO-d_6.

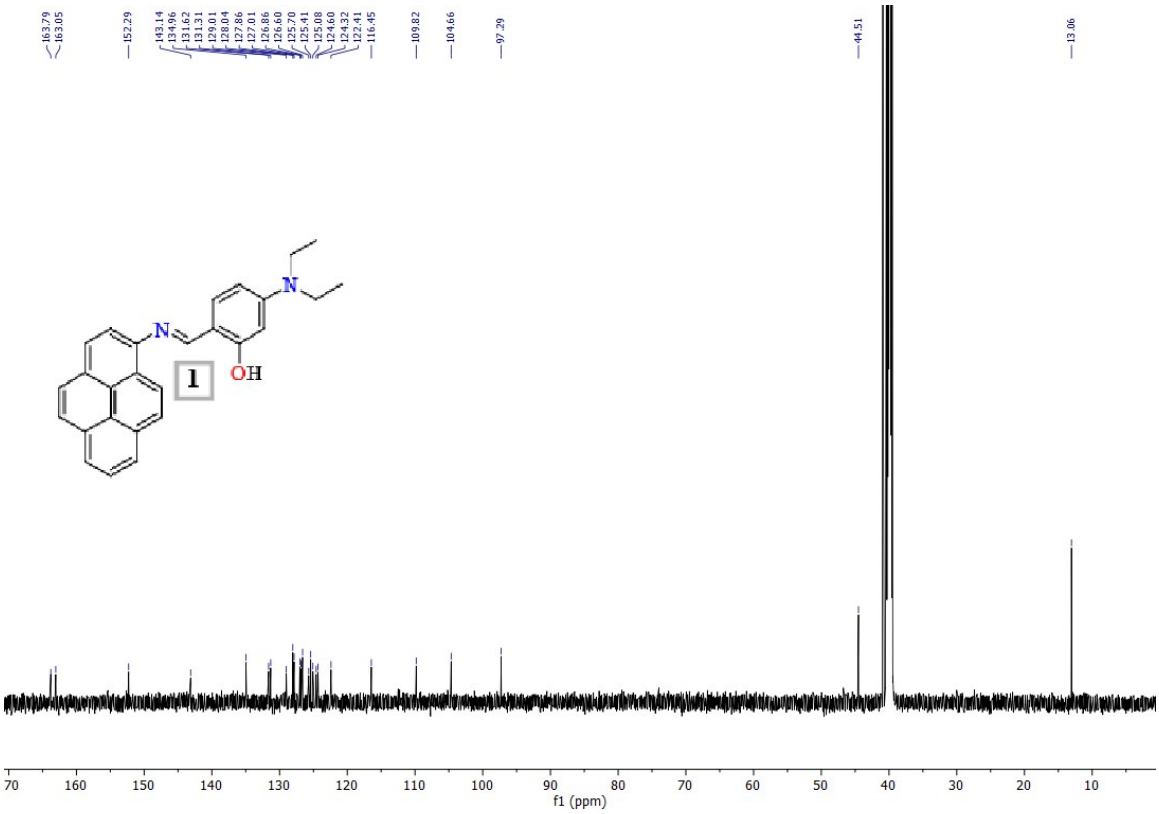

Figure S2: ^{13}C-NMR spectra of **1** in DMSO-d_6.

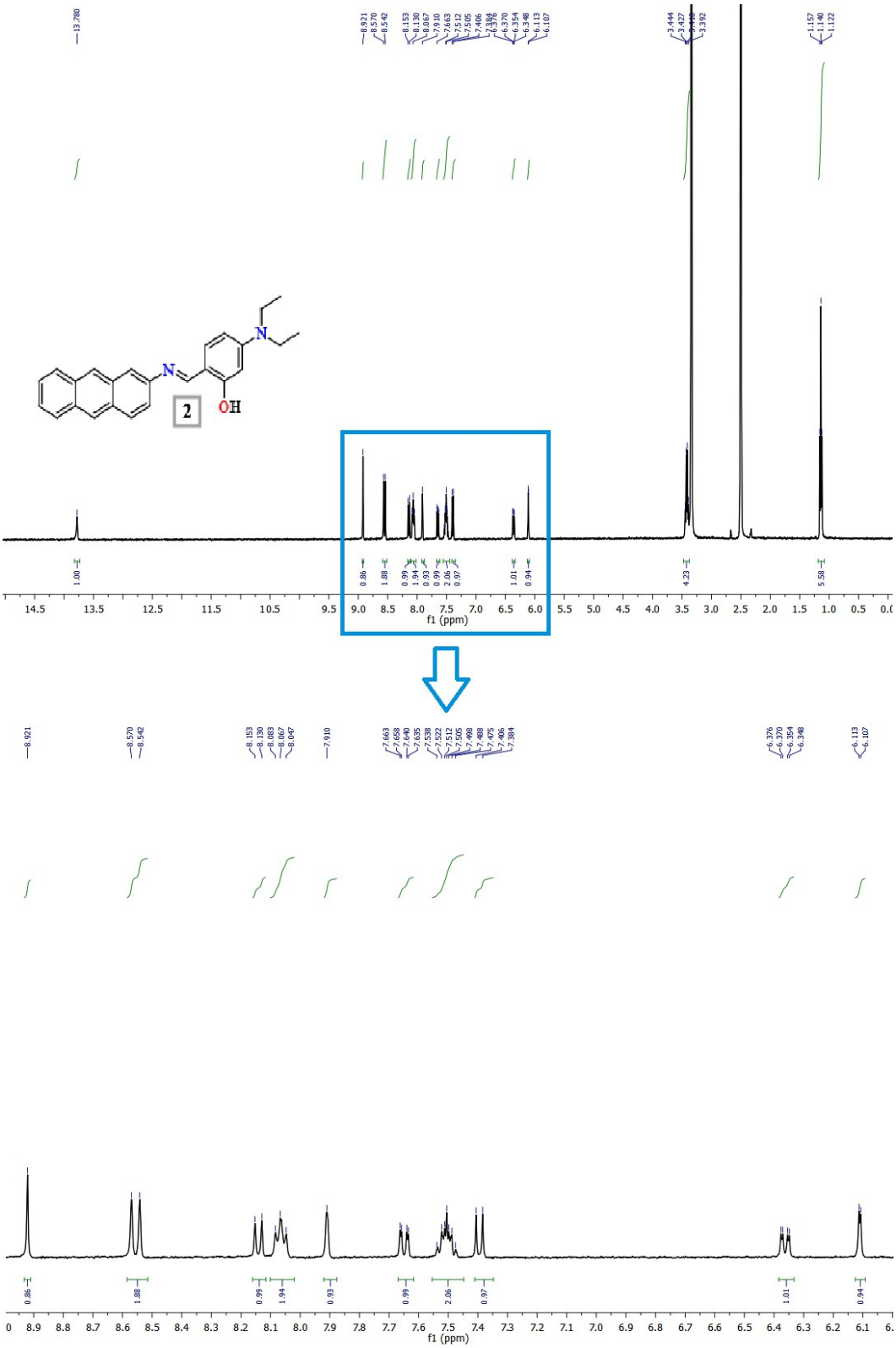

Figure S3: ^{1}H-NMR spectra of **2** in DMSO-d_6.

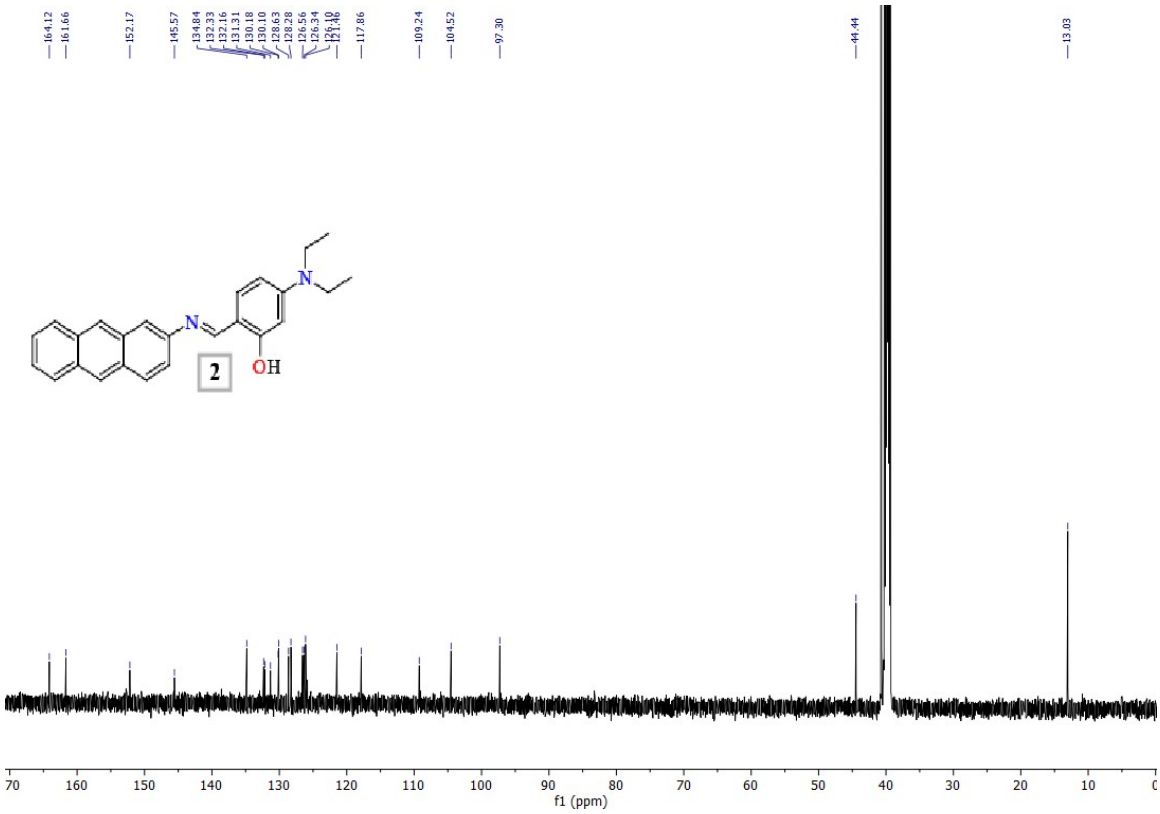

Figure S4: ^{13}C-NMR spectra of **2** in DMSO-d_6.

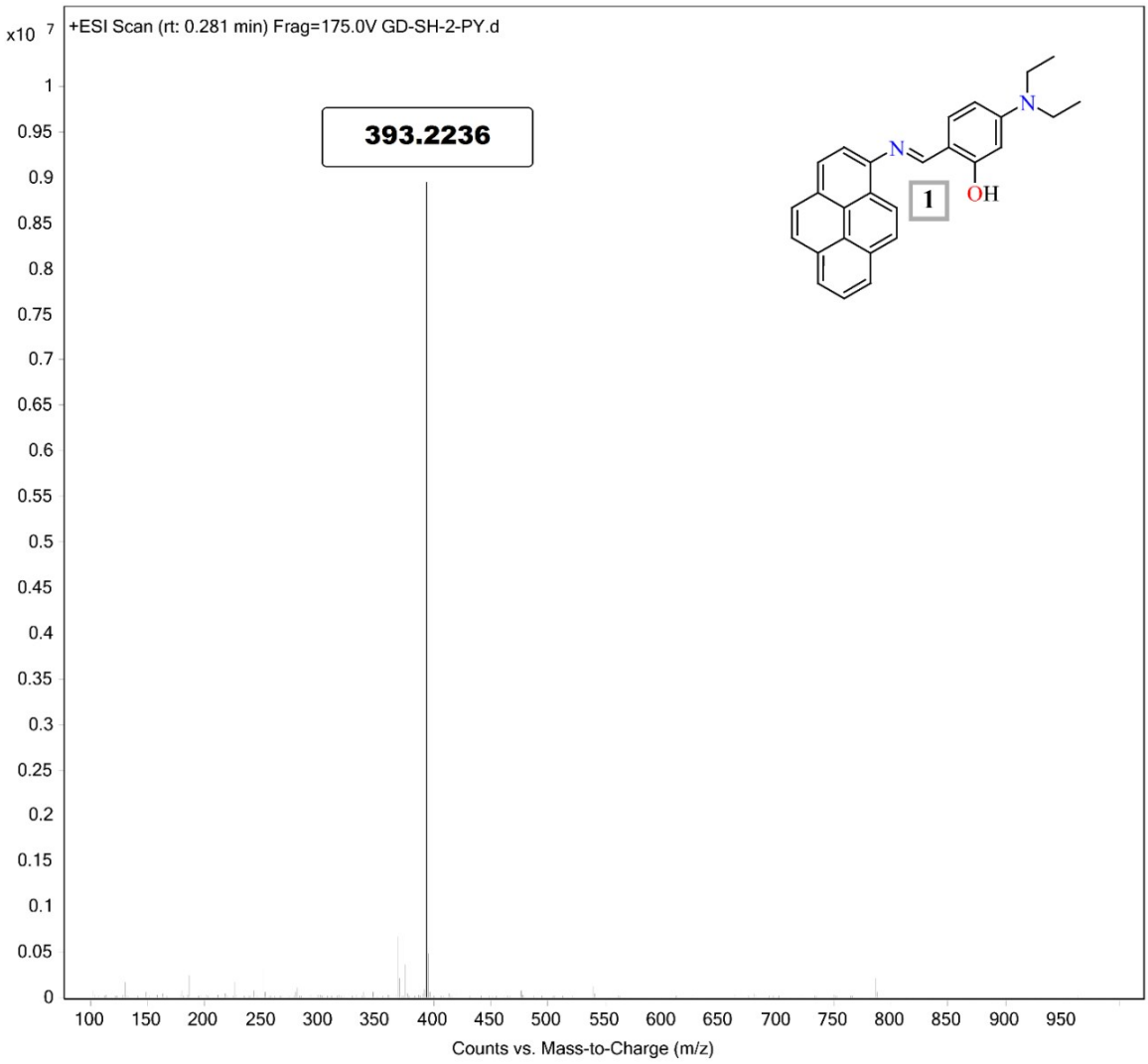

Figure S5: Mass spectrum of **1** (Calculated: 393.1922; Obtained: 393.2236).

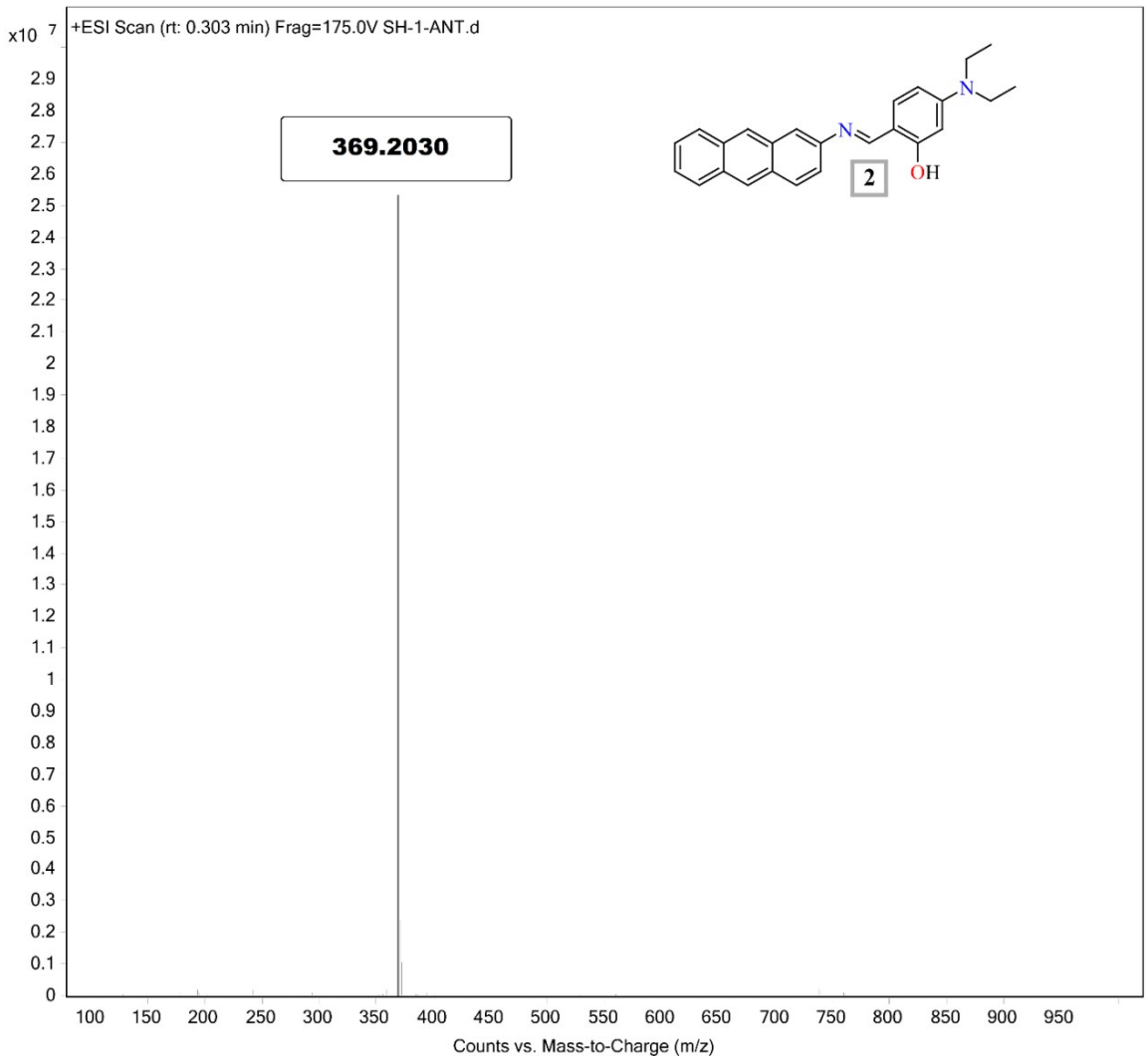

Figure S6: Mass spectrum of **2** (Calculated: 369.1922; Obtained: 369.2030).

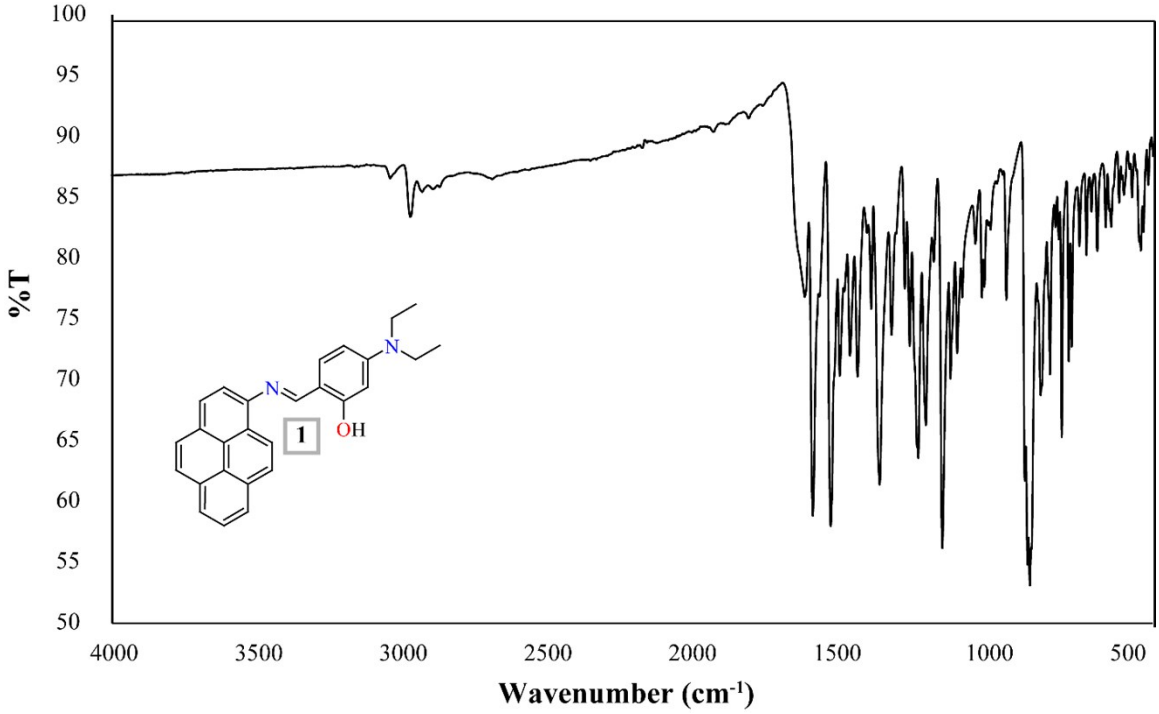

Figure S7: FT-IR spectrum of **1** recorded in KBr pellet at 25ºC.

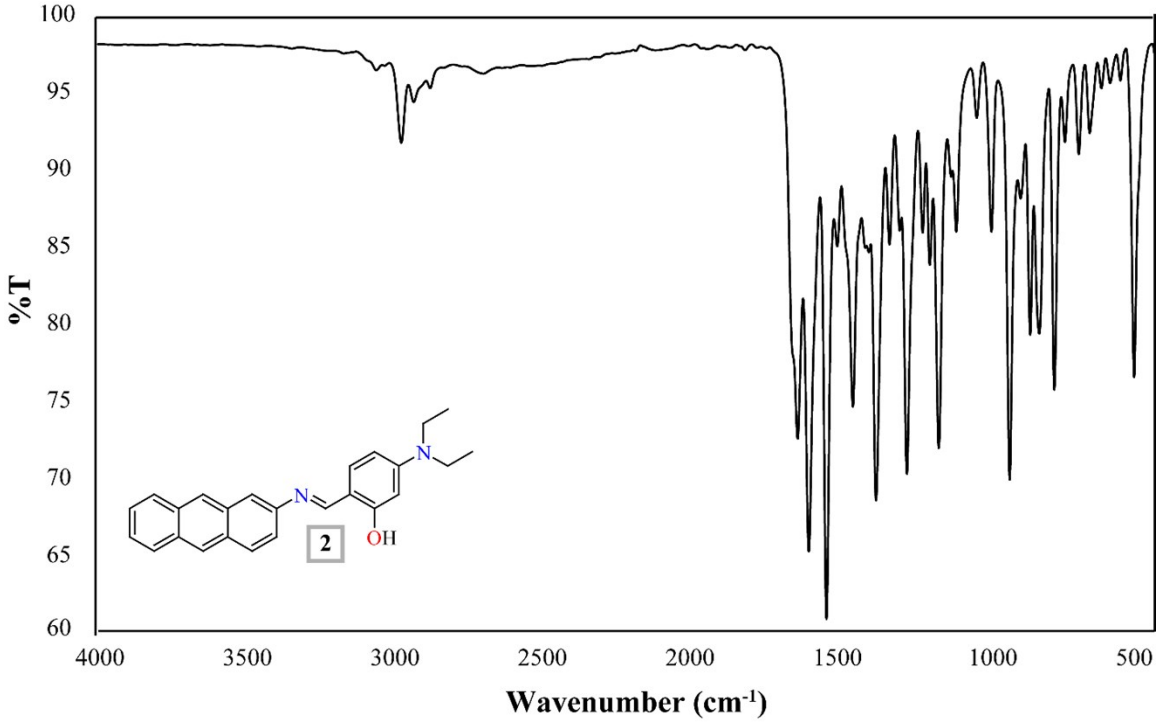

Figure S8: FT-IR spectrum of **2** recorded in KBr pellet at 25ºC.

Table S1: Hydrogen bonding table of **1**.

Ligand	D−H···A	d(D···H)/Å	d(H···A)/Å	d(D···A)/Å	<D−H···A/°	Symmetry codes
	O1-H1···N1	0.82	1.87	2.608(3)	149	x, y, z
	O2-H2···N3	0.82	1.88	2.612(4)	148	x, y, z
	C8-H8···N1	0.93	2.53	2.842(4)	100	x, y, z
	C38-H38···N3	0.93	2.55	2.857(4)	100	x, y, z
	C44-H44···O1	0.93	2.60	3.516(4)	170	x, y, z

Table S2: Quantum yields (□) values of **1** and **2** in different water fractions.

Sample	Quantum Yield (□)
1 (f_w = 0%)	0.0009
1 (f_w = 50%)	0.002
1 (f_w = 100%)	0.006
2 (f_w = 0%)	0.005
2 (f_w = 50%)	0.018
2 (f_w = 100%)	0.004

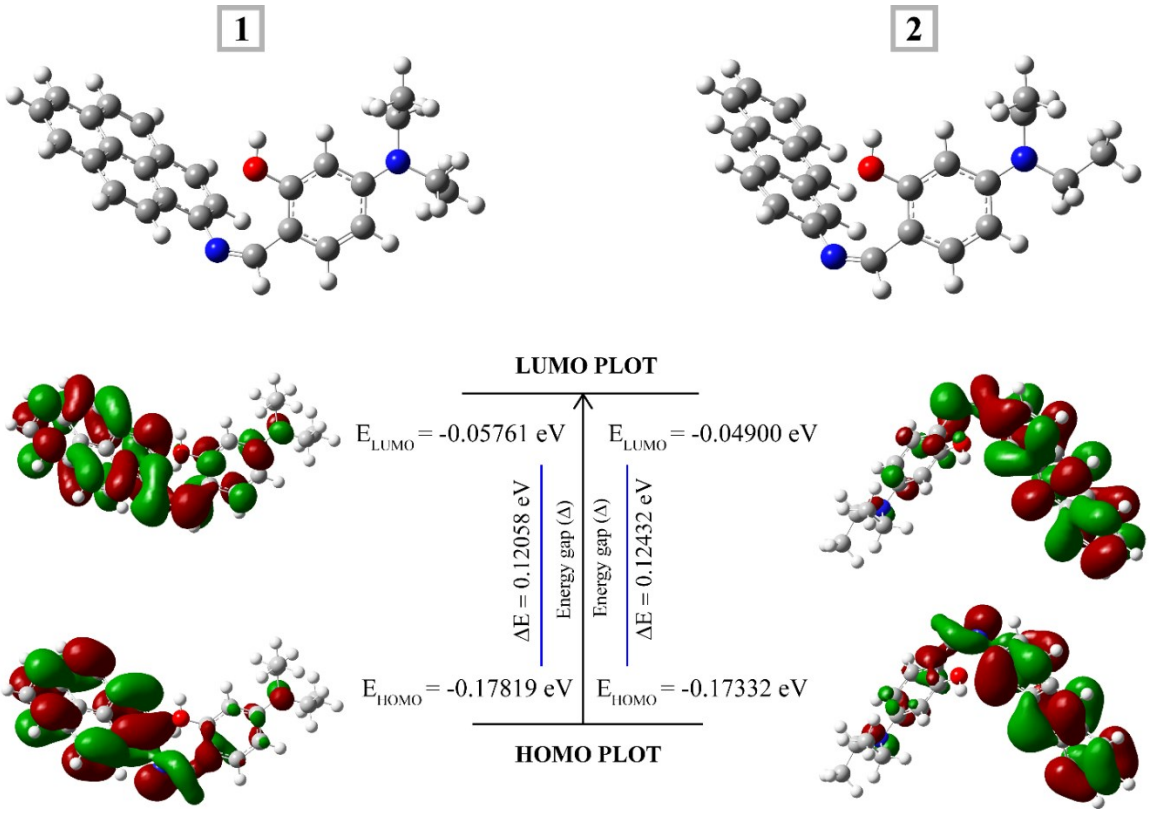

Figure S9: Geometry optimized structures and Frontier molecular orbital plots (ΔE = energy gap between HOMO and LUMO) of **1**(left) and **2**(right) using RB3LYP/6-31G as implemented on Gaussian 09.

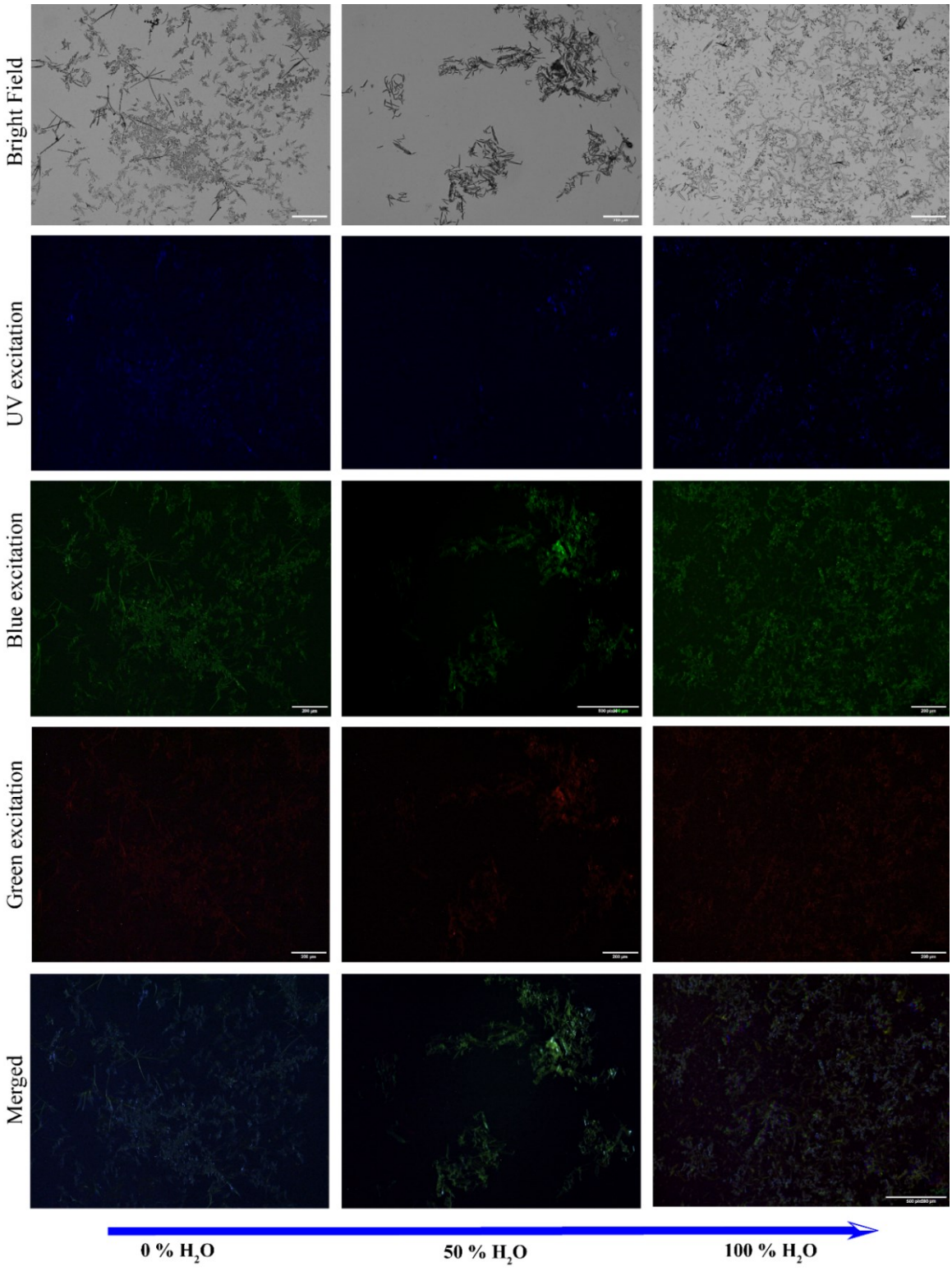

Figure S10: Fluorescence microscope images of **1** at different excitation range by varying the solvent fraction. [Bright field, UV channel (λ_{ex}=404.1 nm, λ_{em} = 425–475 nm) blue channel (λ_{ex}=488 nm, λ_{em} = 500–530 nm), green channel (λ_{ex}=543.5 nm, λ_{em} = 553–618 nm) and merged, scale bar = 200 μm].

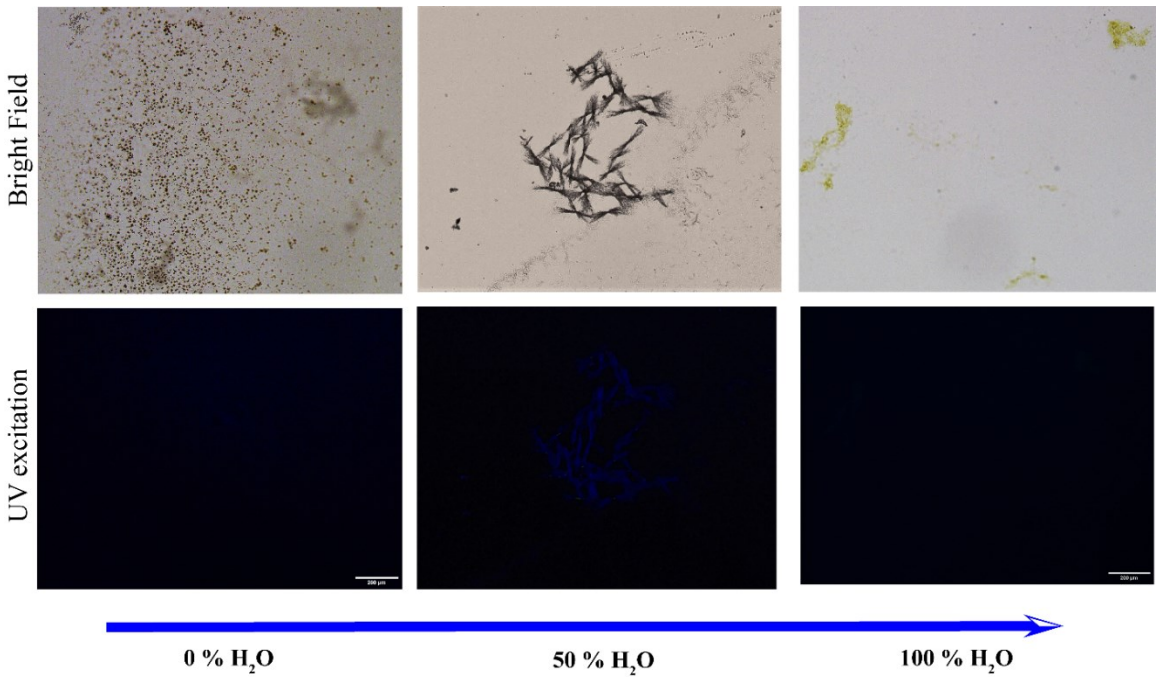

Figure S11: Fluorescence microscope images of **2** by varying the solvent fraction. [Bright field, UV channel (λ_{ex}=404.1 nm, λ_{em} = 425–475 nm), scale bar = 200 µm].

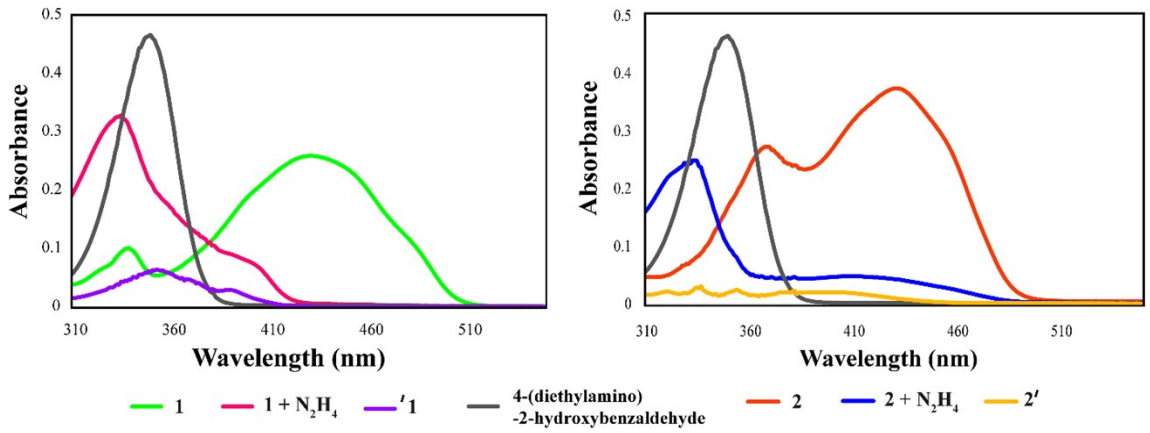

Figure S12: Comparative UV-visible spectra of **1** and **2** in absence and presence of excess hydrazine (10 equiv.) as well as their starting material in 1:1 acetonitrile-water medium.

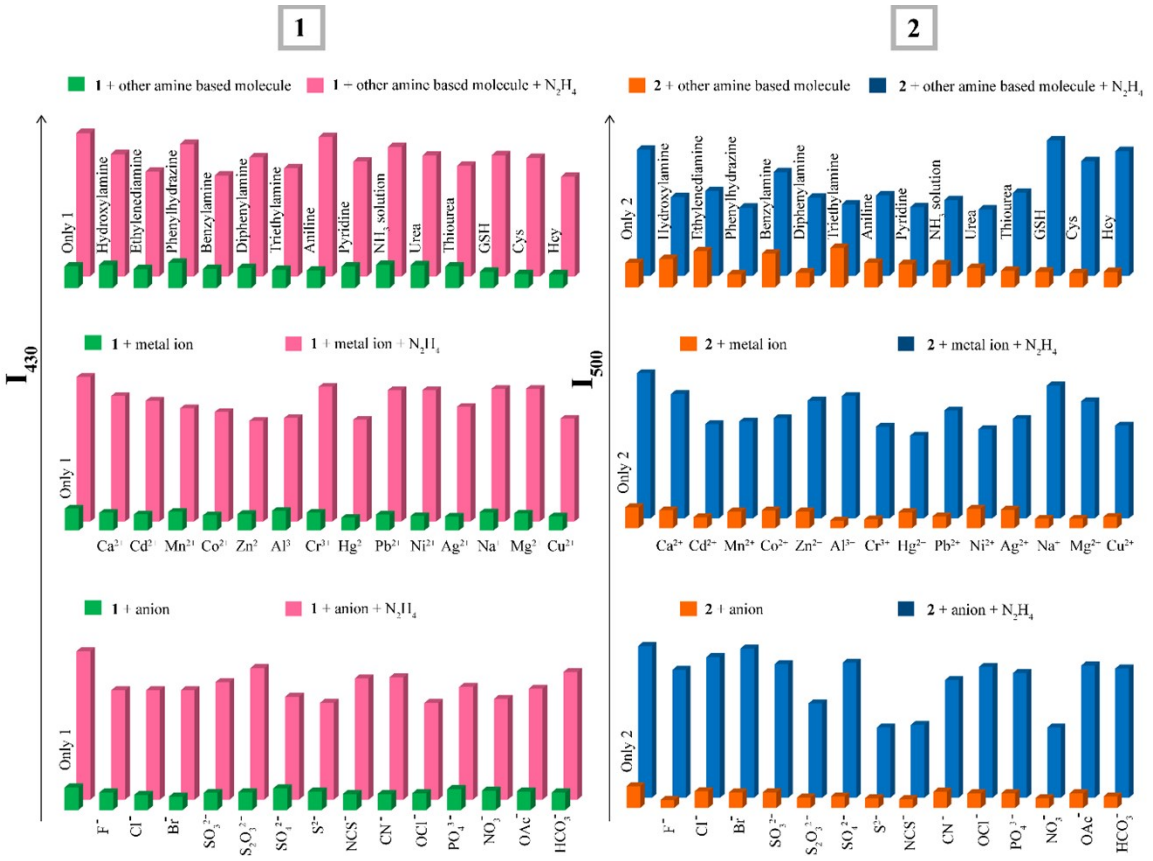

Figure S13: Selectivity of **1** and **2** (10 μM) in 1:1 acetonitrile-water medium in the presence of an excess (10 equivalents) of various amine based compounds, metal ions and anions.

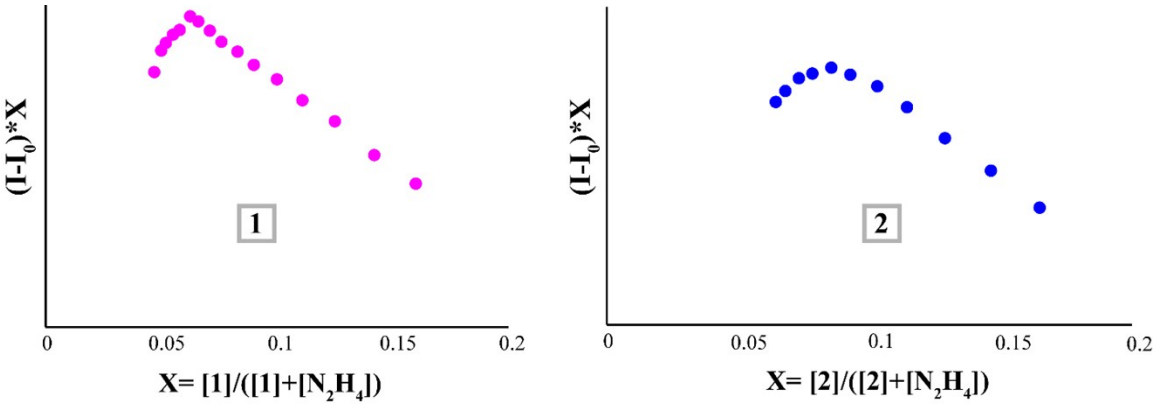

Figure S14: Job's plot obtained from the fluorescence titration experiment of **1** and **2**.

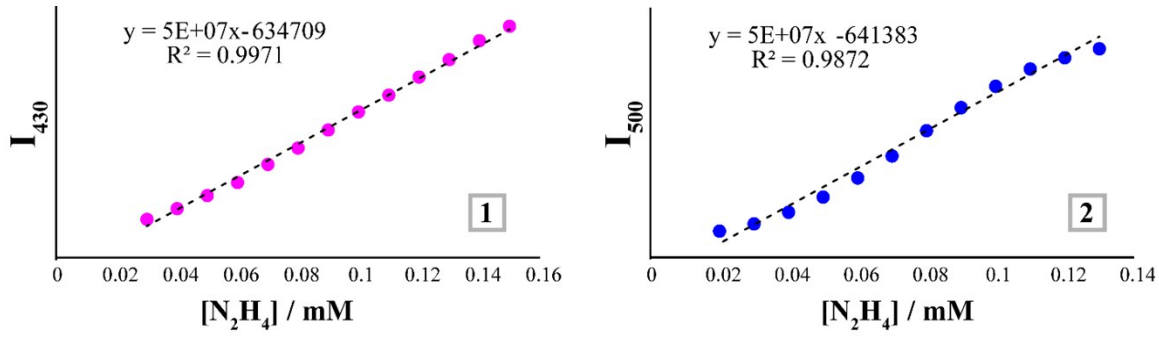

Figure S15: Fluorescence intensity vs. concentration of HSA plot for determination of detection limit.

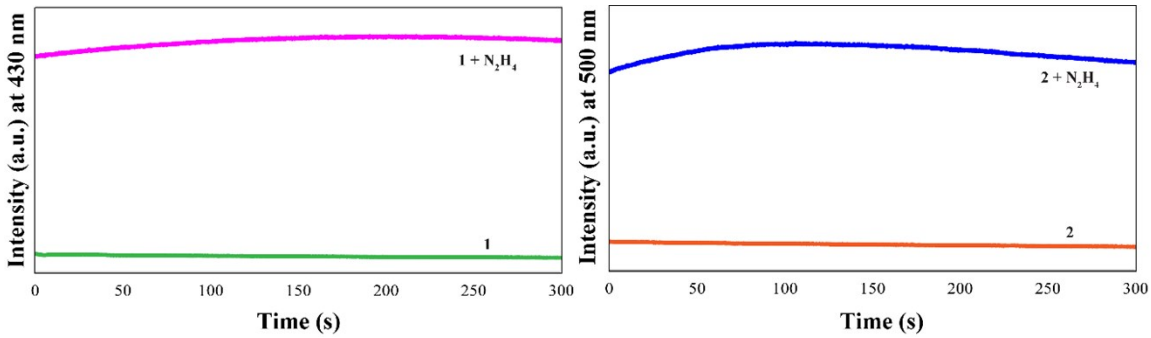

Figure S16: Changes in the emission intensity of **1** and **2** with time upon interaction with hydrazine.

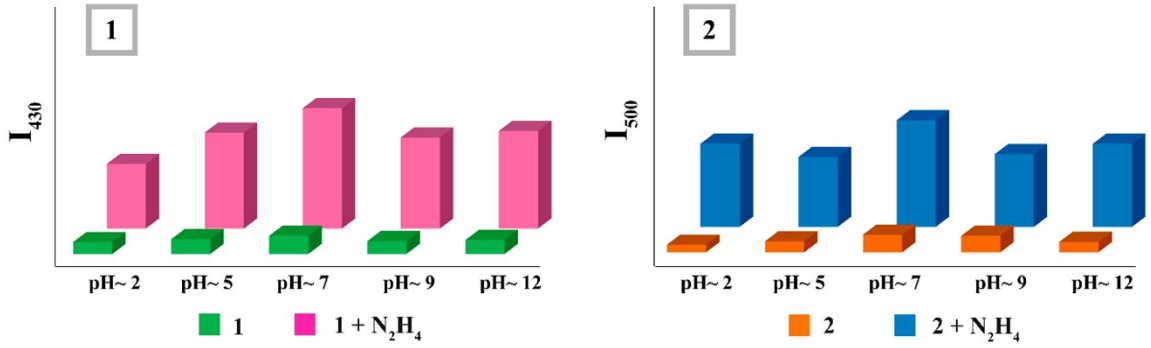

Figure S17: Fluorescence intensity of **1**/**2** and **1**/**2**–N_2H_4 adduct at different pH values at room temperature.

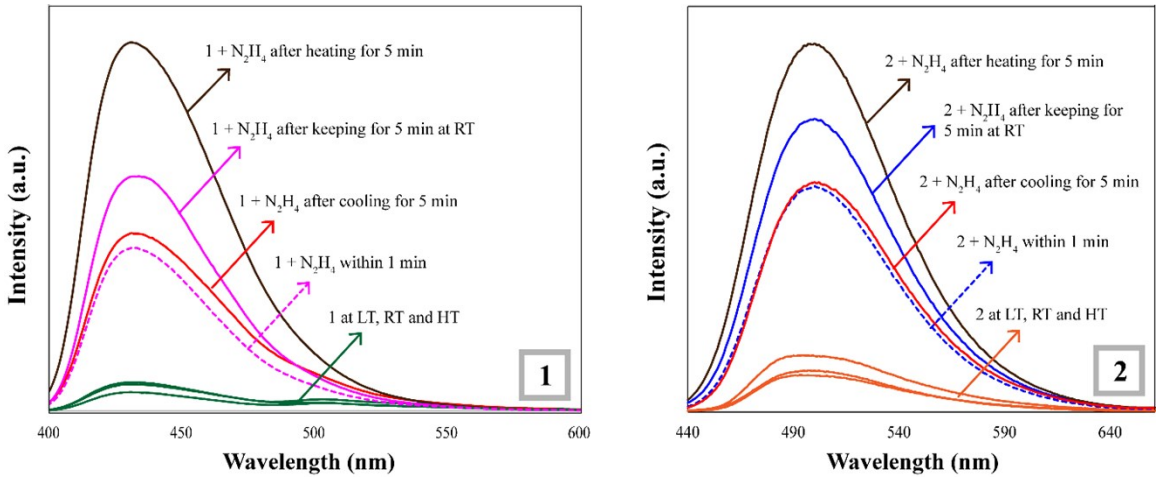

Figure S18: Effect of temperature on emission intensity of **1**/**2** and **1**/**2**–N_2H_4 adduct.

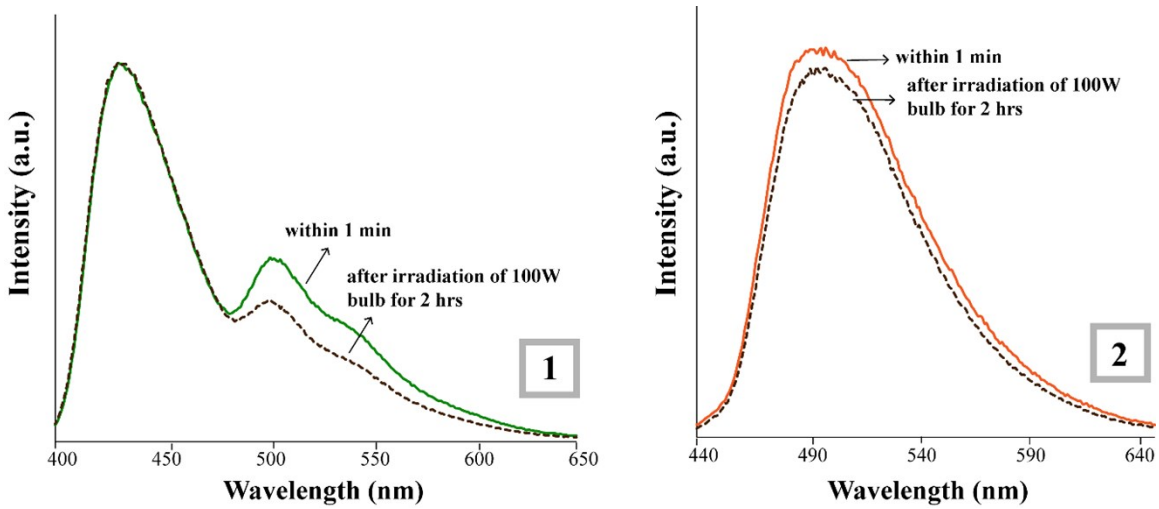

Figure S19: Fluorescence spectra of AIEgens **1** and **2** (10 μM) before and after the irradiation of a 100W bulb for 2 hrs in 1:1 acetonitrile-water medium.

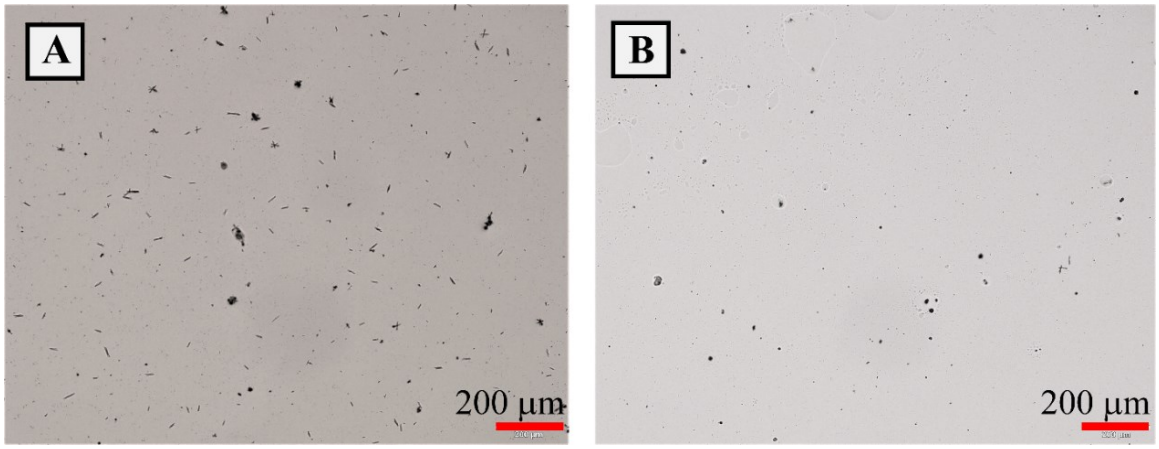

Figure S20: Optical microscope images of AIEgens **1** and **2** after hydrazine addition [Scale bar: 200 µm.].

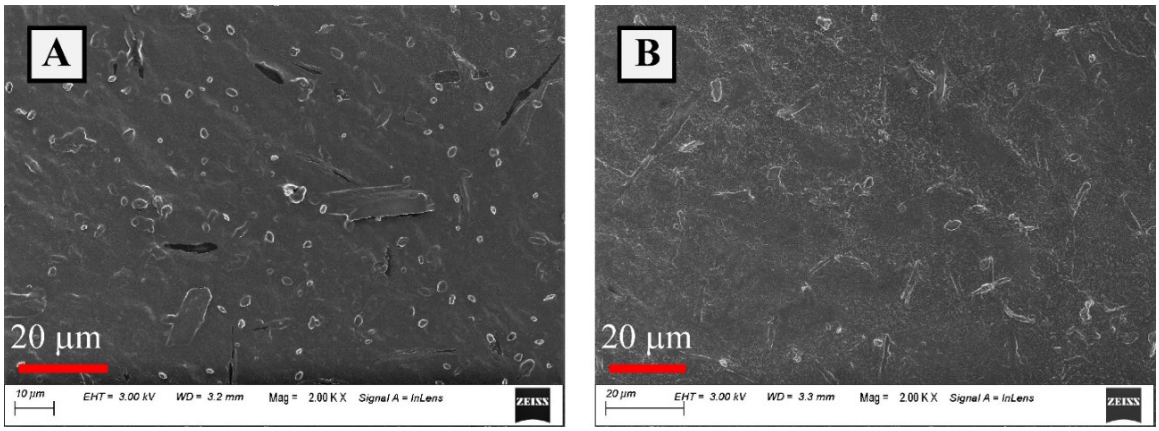

Figure S21: FESEM images of AIEgens **1** and **2** after hydrazine addition [Scale bar: 20 µm].

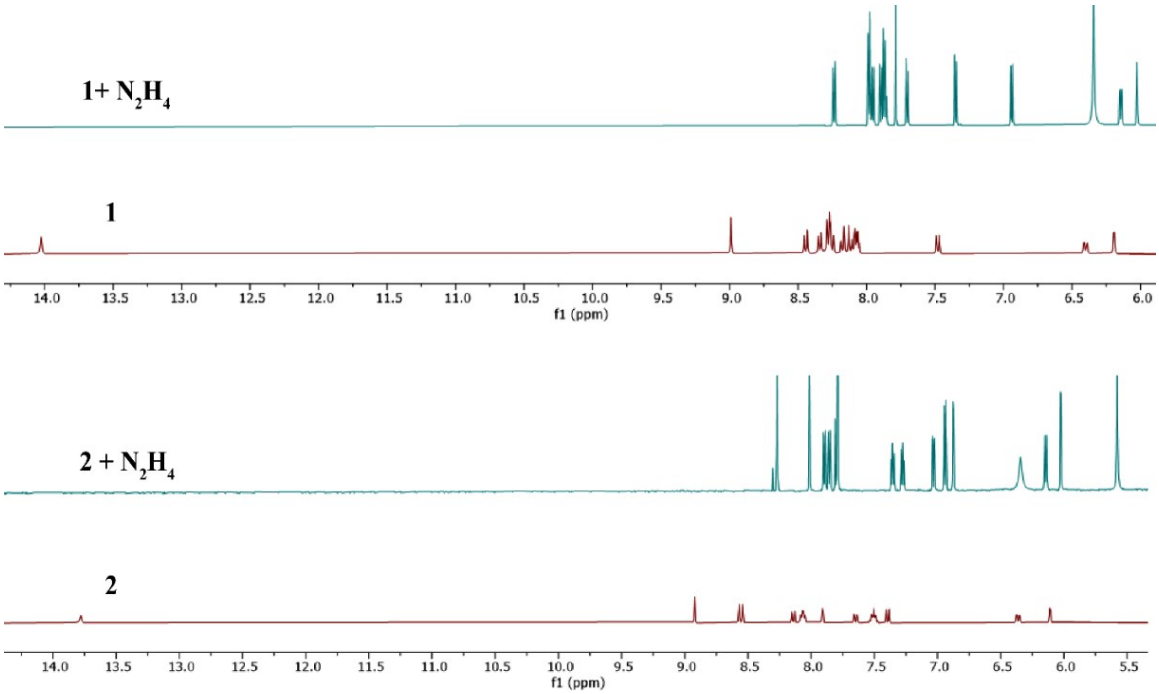

Figure S22: ^{1}H NMR spectra of the **1** and **2** and its N_2H_4 adduct in DMSO-d_6.

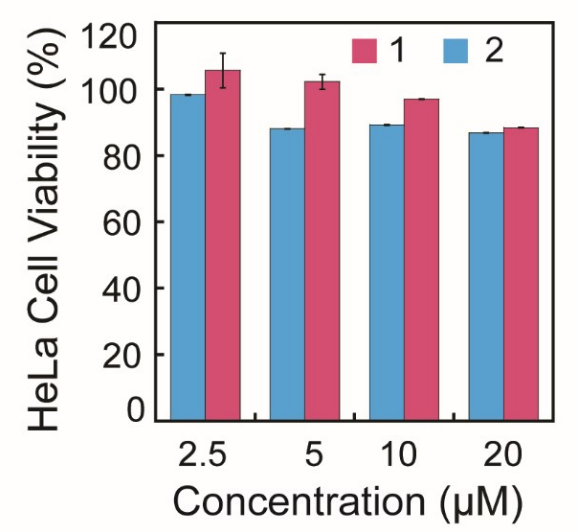

Figure S23: MTT assay to ascertain the cytotoxic effect of the AIEgens **1** and **2** against HeLa cells. Each data point represent mean ± standard deviation from six samples.

Table S3: Comparative study on the recent progress in the field of hydrazine sensing.

Sl. No.	Reference	Fluorophore involved and sensing mode	Solvent system	Detection limit	Application
1.	Dyes Pigm., **2020**, 174, 108056	Naphthalene OFF-ON/-	DMSO	$1.1*10^{-7}$ M	Test strips
2.	Dyes Pigm., **2020**, 175, 108111	Coumarin OFF-ON/ICT, AIE	PBS/DMSO (2/3)	1.29 ppb M	solid state lighting
3.	ACS Sustain. Chem. Eng. **2020**, 8, 4457	Naphthofluorescein OFF-ON	aqueous medium	~47 nM	eco-friendly test strip, bioimaging
4.	ACS Sens. **2019**, 4, 441	orthomethoxy-methyl-ether OFF-ON	DI H_2O	0.035 ppb	spray-based sensing, soil analysis, and bioimaging in tissue samples
5.	Sens. Actuators B Chem., **2019**, 285, 368–374	1, 8-Naphthalimide ratiometric	PBS/DMSO (1:1)	$2.03*10^{-7}$	Filter paper strips, HepG-2 cells
6.	Org. Biomol. Chem., **2019**, 17, 6975–6979	Schaap's Adamantylidene–dioxetane OFF-ON/Chemiluminescent	PBS/DMSO (7:3)	$9.3*10^{-7}$ M	water samples/HeLa cells
7.	Int. J. Environ. Anal. Chem., **2019**, 1–13	Imidazo [1,5-a] pyridin OFF-ON/ESIPT	PBS/DMSO (10:1)	2.56 ppb	test strips, HeLa cells
8.	Sens. Actuators B Chem., **2018**, 272. 479–484	Triphenylamine ON-OFF/self-assemble	PBS buffer	-	Hela cells
9.	Anal. Chem. **2017**, 89, 10625	1-Pyrenecarboxaldehyde and 9-anthraldehyde OFF-ON/-	H_2O/CH_3OH(4:1)	5.4, 7.7 ppb	Drosophila larvae, paper test strips,MCF-7 cells
10.	Present Work	Pyrene and anthracene based Schiff base OFF-ON/hydrogen bonding	ACN/H_2O (1:1)	0.5, 0.4 ppb	test strips, water samples, plant imaging

References:

[1] G.M. Sheldrick, SAINT and XPREP, 5.1 ed., Siemens Industrial Automation Inc., Madison, WI, 1995.

[2] G.M. Sheldrick, SADABS: Software for Empirical Absorption Correction, University of Gottingen, Institute fur Anorganische Chemieder Universitat, Tammanstrasse 4, D-3400 Gottingen, Germany, 1999-2003.

[3] G.M. Sheldrick, SHELXS-97, University of Gottingen, Germany, 1997.

[4] G.M. Sheldrick, SHELXL-97, Program for Crystal Structure Refinement, University of Gottingen, Germany, 1997.

[5] Mercury 1.3 Supplied with Cambridge Structural Database, CCDC, Cambridge, U.K., 2003-2004.